https://doi.org/10.2352/issn.2169-2629.2020.28.29

Improved camera color accuracy in the presence of noise with a color prefilter

Michael J. Vrhel, Artifex Software, 1305 Grant Avenue, Suite 200, Novato, CA 94945

Abstract

It is possible to achieve improved color accuracy with a color camera by placing a color filter in front of the camera. Unfortunately, the color filter will block some of the light entering the camera, which will result in additional noise in the recorded data. This paper provides an initial investigation into finding an optimal solution to the filter design, in the presence of noise.

Introduction

Over the years, there have been a number of papers dealing with the problem of designing or creating color filters for cameras and scanners. In some papers, the focus has been to optimize for spectral discrimination rather than colorimetry [1, 2, 3, 4, 5].

Early examples of filter design and selection focused on colorimetry include [6, 7, 8]. The references [9, 10] considered the effect of noise in the optimization problem. The later work by Kuniba [11] looks at the problem of filter design in the presence of shot noise. Wolski [12] introduced the idea of including a Taylor series approximation of the transformation to CIELAB in the optimization problem to achieve improved perceptual color performance. Considerations for realizability are made in [13]. The work by Parmar [14] considers the practical impact of the color filter array into the problem of filter design. Work by Trussell [15] investigated the use of a large number of narrow band filters in the presence of Poisson noise.

The work by Vora and Trussell [16, 17] went into details on analyzing and quantifying the effect of variations on color filters as well as coming up with a measure of goodness for a set of filters [18], which has been termed the Vora value. This measure is a multi-dimensional generalization of Neugebauer's q-factor [19]. Sharma [20] pushed the idea of a measure of goodness further by introducing a Taylor series approximation of the transformation to CIELAB as well as introducing noise into the measure. Quan [21] also introduces a measure of goodness when designing filter responses. Further generalization of figures of merits are made in [22].

Recently there have been a number of papers that have looked at the idea of achieving improved color accuracy of an existing camera by placing a color filter in front of the camera [23, 24, 25]. This color filter alters the overall spectral sensitivity of the camera. If the filter is carefully designed, it is possible to achieve a closer approximation to the subspace spanned by the CIEXYZ color matching functions. One problem with this approach is that any filter that blocks light will result in a system that has a lower signal-to-noise ratio. While one can always assume that they could increase the light level to achieve any desired SNR, there will always be noise present in the recording process and it really should be considered in the optimization problem.

Here we take a look at the problem of noise in this filter optimization process. The approach is to make use of a figure of merit developed by Sharma, as it already includes considerations for noise. Comparisons are made to a method that does not take noise into consideration in the filter design process.

Mathematical notation

If we assume we can mathematically sample the visible spectrum at a sufficient number of wavelengths, n, to allow an accurate representation of the spectral information [26], we can model the camera color imaging system using a vector notation. The imaging model is given by

$$\mathbf{c}_i = \mathbf{H}^T \mathbf{r}_i + \mathbf{n}_i, \tag{1}$$

where the columns of the nxm matrix $\mathbf{H}$ define the m spectral separation channels for the camera[1], the n-element vector $\mathbf{r}_i$ represents the variable radiant spectrum at pixel location i, the m-element vector $\mathbf{n}_i$ represents the additive noise at location i, and $\mathbf{c}_i$ is the m-element vector obtained with the camera at location i. Note that we have used a single index i for the location for simplification.

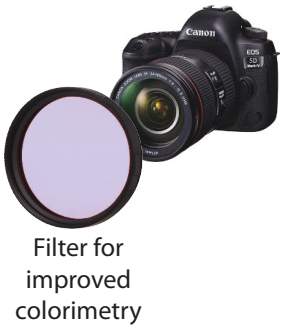

Figure 1. *Prefilter placed in front of digital camera to improve colorimetry of camera.*

The problem posed is that we wish to place a filter in front of the camera to achieve improved colorimetry as graphically shown in Figure 1. Ideally the complete camera response would be within a linear transformation of the CIEXYZ color matching functions, which is to say that it would satisfy the Luther condition [27]. In general, it is difficult to achieve this goal, but given some recorded data with our camera we wish to obtain an estimate of the CIEXYZ value of the spectrum $\mathbf{r}_i$, which is mathematically expressed as

$$\mathbf{t}_i = \mathbf{A}^T \mathbf{r}_i, \tag{2}$$

[1] In most cases $m = 3$.

where the columns of the matrix **A** are the sampled CIEXYZ color matching functions.

There are a number of ways to obtain such an estimate. To simplify things, and focus instead on the filter optimization problem, we will use a linear estimator and in particular the linear minimum mean square error estimator since we can readily compute this matrix analytically. This matrix, $\mathbf{B}_{lmmse}$ is the solution to the optimization problem

$$\mathbf{B}_{lmmse} = \arg\min_{\mathbf{B}} E\left\{||\mathbf{t}-\mathbf{Bc}||^2\right\} \tag{3}$$

and the estimated CIEXYZ tristimulus value is given by

$$\hat{\mathbf{t}}_i = \mathbf{B}_{lmmse}\mathbf{c}_i. \tag{4}$$

The solution to Equation 3 is given by

$$\mathbf{B}_{lmmse} = \mathbf{A}^T\mathbf{K}_r\mathbf{H}(\mathbf{H}^T\mathbf{K}_r\mathbf{H}+\mathbf{K}_n)^{-1} \tag{5}$$

where

$$\mathbf{K}_r = E\left\{\mathbf{r}\mathbf{r}^T\right\} \tag{6}$$

is the correlation matrix of the radiant spectra seen by the camera and

$$\mathbf{K}_n = E\left\{\mathbf{n}\mathbf{n}^T\right\} \tag{7}$$

is the noise covariance matrix, assuming the noise is zero mean.

Mathematically, the insertion of the filter into the optical path can be modeled as

$$\mathbf{c}_i = \mathbf{H}^T\mathbf{F}\mathbf{r}_i + \mathbf{n}_i, \tag{8}$$

where **F** is an *n*x*n* diagonal matrix whose diagonal elements represent the spectral transmittance of the filter. We will denote the filter transmittance also as the *n*-element vector **f** where $\text{diag}(\mathbf{f}) = \mathbf{F}$.

Figures of merit

The problem of finding the optimal filter can be approached a number of ways. One method is to consider figures of merits that provide a measure of how well the spectral sensitivity of the entire system can cover the subspace defined by the spectral sensitivity of the standard human observer. One such measure is the Vora value [18] given by

$$\nu(\mathbf{A},\mathbf{FH}) = \frac{\text{Trace}\left[\mathbf{A}(\mathbf{A}^T\mathbf{A})^{-1}\mathbf{A}^T\mathbf{FH}((\mathbf{FH})^T\mathbf{FH})^{-1}(\mathbf{FH})^T\right]}{3}, \tag{9}$$

which is the trace of the product of the orthogonal projection operator onto the subspace defined by the CIEXYZ color matching functions and the orthogonal projection operator onto the subspace defined by our camera's spectral sensitivity, divided by three. The measure is bounded between zero and one, with zero meaning that the subspace spanned by the camera spectral sensitivity **FH** is in the null space of matrix **A** and one meaning that the spectral sensitivities cover the subspace spanned by the matrix **A**. If we have a measure of one, then it is possible to obtain CIEXYZ values using the filter set **FH**. The optimization problem would thus be to find a diagonal matrix **F** that will maximize $\nu(\mathbf{A},\mathbf{FH})$.

A downside of this approach is that it takes in no consideration of the impact of the noise term in Equation 8. One of the figure of merits developed by Sharma [20] that factors in the noise term is expressed as

$$q(\mathbf{A},\mathbf{FH},\mathbf{K}_r,\mathbf{K}_n) = \frac{\tau(\mathbf{A},\mathbf{FH},\mathbf{K}_r,\mathbf{K}_n)}{\text{Trace}\left[\mathbf{P}_\mathbf{A}\mathbf{K}_r\right]} \tag{10}$$

where

$$\tau(\mathbf{A},\mathbf{FH},\mathbf{K}_r,\mathbf{K}_n) = \text{Trace}\left[\mathbf{P}_\mathbf{A}\mathbf{K}_r\mathbf{FH}\left(\mathbf{H}^T\mathbf{F}\mathbf{K}_r\mathbf{F}\mathbf{H}+\mathbf{K}_n\right)^{-1}\mathbf{H}^T\mathbf{F}\mathbf{K}_r\right], \tag{11}$$

and the term $\mathbf{P}_\mathbf{A}$ is given by

$$\mathbf{P}_\mathbf{A} = \mathbf{A}(\mathbf{A}^T\mathbf{A})^{-1}\mathbf{A}^T \tag{12}$$

which is the orthogonal projection operator onto the subspace defined by the CIEXYZ color matching functions.

Similar to the Vora value, the measure $q(\mathbf{A},\mathbf{FH},\mathbf{K}_r,\mathbf{K}_n)$ has a minimum of zero and a maximum value of one. Note that in his work, Sharma defines a number of measures including those that provide a first order Taylor series approximation to the mapping to CIELAB from CIEXYZ. Here though we are interested in focusing only upon the effects of noise in our filter selection.

Correlation, Noise and SNR

The radiant spectra correlation matrix $\mathbf{K}_r$ can be derived from a collection of radiant spectra such as that provided by Wueller [28]. This data set consists of over 2000 samples of various object spectra recorded in-situ with a spectroradiometer. If the data of the Wueller spectra are contained in the columns of the matrix **G** where

$$\mathbf{G} = [\mathbf{r}_1,\ldots,\mathbf{r}_s] \tag{13}$$

then an estimated covariance matrix would be given by

$$\mathbf{K}_{data} = \frac{1}{s}\mathbf{G}\mathbf{G}^T. \tag{14}$$

where *s* is the number of samples in the data set.

Alternatively, to avoid the use of the exact statistics of which we are going to assess performance (and focus only on signal-to-noise ratio), we can assume a correlation matrix that uses a fixed correlation ρ between adjacent samples in the spectrum, and a power level (or variance) at each wavelength that is the same as the matrix $\mathbf{K}_{data}$. If the correlation between adjacent wavelengths is given by ρ, such a matrix would be expressed as

$$\mathbf{K}_{model} = [\text{diag}\,(\mathbf{K}_{data})]^{1/2}\,\mathbf{M}\,[\text{diag}\,(\mathbf{K}_{data})]^{1/2} \tag{15}$$

where $\text{diag}\,(\mathbf{X})$ is a diagonal matrix with the same diagonal elements as **X** and

$$\mathbf{M} = \begin{bmatrix} 1 & \rho & \rho^2 & \rho^3 & . & . & . & \rho^{n-1} \\ \rho & 1 & \rho & \rho^2 & . & . & . & \rho^{n-2} \\ . & . & . & . & . & . & . & . \\ . & . & . & . & . & . & . & . \\ . & . & . & . & . & . & . & . \\ \rho^{n-1} & \rho^{n-2} & . & . & . & . & . & 1 \end{bmatrix}. \tag{16}$$

If we assume the noise is zero-mean white Gaussian noise then we can express the noise covariance matrix as

$$\mathbf{K}_n = \sigma_n^2 \mathbf{I} \tag{17}$$

where the noise variance is given by σ_n^2. It should be noted that a Poisson signal-dependent noise model is likely more appropriate as described in [29], but at this time we will focus on the signal-independent Gaussian case.

The signal-to-noise ratio (SNR) can be defined as

$$\text{SNR(dB)} = 10\log_{10}\left(\frac{\text{Trace}\left[\mathbf{H}^T\mathbf{F}\tilde{\mathbf{K}}_r\mathbf{F}\mathbf{H}\right]}{\sigma_n^2}\right). \tag{18}$$

where the estimated covariance matrix $\tilde{\mathbf{K}}_r$ is $\mathbf{K}_{data}$ or $\mathbf{K}_{model}$.

Filter Model

To be realizable, the filter transmittance should be bounded between zero and one at each wavelength. In addition, we would like the filter to be a smooth function of wavelength. To enforce the smoothness constraint, it is simple to model the filter transmittance as a weighted sum of piece-wise cubic Hermite interpolating polynomials. This is similar to an approach in [16], which used a weighted sum of Gaussian forms.

Using the Hermite interpolating polynomials, the filter transmittance is given by

$$\mathbf{f} = \mathbf{B}\mathbf{w} \tag{19}$$

where the columns of the matrix $\mathbf{B}$ contain the sampled polynomials and a simple bounding constraint of zero to one on the elements of $\mathbf{w}$ provides us with a smooth bounded filter representation. Figure 2 shows an example curve with its weighted basis functions.

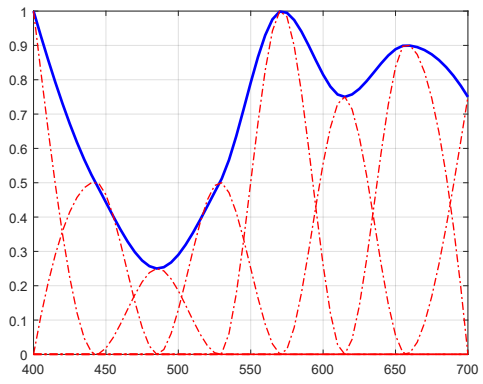

Figure 2. *Smoothness constraint for filter enforced through use of interpolating basis.*

Optimization formulations

Constrained optimization problems to maximize the figure of merit measures $v(\mathbf{A},\mathbf{FH})$ and $q(\mathbf{A},\mathbf{FH},\mathbf{K}_r,\mathbf{K}_n)$ can be readily coded using the fmincon function in MATLAB. Mathematically, the problem can be expressed as

$$\mathbf{f}_v = \arg(\max_{\mathbf{w}}[v(\mathbf{A},\mathbf{FH})]) \tag{20}$$

or

$$\mathbf{f}_q = \arg(\max_{\mathbf{w}}[q(\mathbf{A},\mathbf{FH},\mathbf{K}_r,\mathbf{K}_n)]) \tag{21}$$

where the elements of $\mathbf{w}$ are bounded between zero and one,

$$\mathbf{F} = \text{diag}(\mathbf{B}\mathbf{w}), \tag{22}$$

and $\text{diag}(\mathbf{x})$ creates a diagonal matrix from the vector $\mathbf{x}$. Optimization using fmincon in MATLAB is achieved by negating the above cost functions. Note that the solution $\mathbf{f}_q$ will depend upon the matrices $\mathbf{K}_r$ and $\mathbf{K}_n$ and hence the SNR.

Results

Let us model our filter using eight weighted basis functions, similar to what is shown in Figure 2. Consider now if we have a camera with spectral sensitivities as shown in Figure 3, which were measured from a Nikon D90 camera. Given this set of filters, we solve Equation 20 to find the optimal insertion filter that will maximize the Vora value. The initial filter response selected in the optimization process is a filter with a transmittance of 0.5 at all wavelengths. Similarly, optimal filters were found using Equation 21 for unfiltered SNRs of 40dB, 50dB and 60dB. For each SNR, optimal filters were found using an estimate for $\mathbf{K}_r$ based upon Equation 14 ($\mathbf{K}_{data}$) for the data set given in [28] as well as Equation 15 ($\mathbf{K}_{model}$) with $\rho = 0.9952$, which was determined in a least squares fit to $\mathbf{K}_{data}$. The results are shown in Figures 4-10. Looking at the differences in the optimal filters for the different noise levels, it makes sense that the optimal filter starts to approach an all pass filter as the SNR decreases, indicating the importance of letting in additional signal at the cost of not approximating the CIEXYZ color matching functions as well.

Using each of the these filters, the data given in [28] was mathematically measured with the camera response and the filter with 1000 noise realizations for every sample. The average CIELAB ΔE as well as the mean squared error in the orthogonalized subspace defined by the CIEXYZ color matching functions were computed. The results are shown in Tables 1 and 2. The lmmse estimator (similar to Equation 5) was used to transform the simulated recorded data to orthogonalized CIE values, which were then transformed to CIELAB. Besides being used for the optimization of Equation 21, matrix $\mathbf{K}_r$ in Equation 5 was either $\mathbf{K}_{model}$ or $\mathbf{K}_{data}$ as denoted in Tables 1 and 2. The noise variance was kept the same regardless of the insertion filter. This has the effect of causing a lower SNR in the system due to the insertion filter blocking more of the signal energy. The true resulting SNR that occurs due to the insertion of the filter is given in Table 3.

The data in Tables 1 and 2 is organized in rows for each filter case, with testing done without the use of a filter (No filter), with the filter found by optimizing the Vora value (Vora filter), and the filters that were designed with specific noise variance levels (40dB filter, 50dB filter, and 60dB filter). The columns are organized to separate the different $\mathbf{K}_r$ and SNR cases. In Table 1, the lowest mean squared error for each SNR is denoted in bold red text. Note that regardless of the $\mathbf{K}_r$ matrix that is used, the filters that were

designed for that particular SNR resulted in the lowest error. Table 2 provides the average CIELAB ΔE difference across the data set with the 1000 noise realizations. Due to the nonlinear relationship of the mapping between CIEXYZ and CIELAB, the minimum errors are not always obtained with the noise optimized filters. However, for SNR levels at 50dB and below, the noise optimized filters do better than the Vora filter, which did not account for noise. At the lower SNRs the use of no filter provided the best results.

The data in Table 3 indicates that the Vora filter results in approximately a 5dB loss in SNR, the 40dB filter is approximately a 0.5dB loss, the 50dB filter is approximately a 2dB loss and the 60dB filter is approximately a 6dB loss. It is interesting to note that by 60dB SNR we are allowing an even greater loss in SNR compared to the Vora filter, but achieving a better mean squared error. In this case, the noise filter is taking advantage of how the SNR is distributed spectrally to ensure an even better capture of data compared to the Vora filter, which is essentially assuming a spectral covariance matrix that is equal to the identity matrix and a noise covariance matrix that is the zero matrix.

It is worthwhile to compare the 60dB SNR results here with the results in [23], which made use of the Vora value, a number of digital cameras and a linear transformation that was a least squares mapping to transform the camera response to the CIEXYZ color matching functions. Finlayson used a different spectral data set to assess performance, but the results are of a similar magnitude with the results here. For the work here, Table 2 shows an improvement from 1.50 ΔE with no filter to a value of 1.04 ΔE with the Vora filter. Finlayson's average improvement over all his cameras went from about 1.3 to 1.0 ΔE. [2]

The author would like to thank Dietmar Wüller for providing access to his data base of spectral radiant measurements.

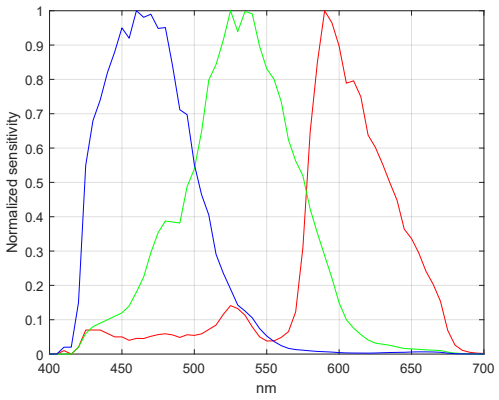

Figure 3. *Camera spectral sensitivities*

[2]The actual values are not provided in [23], but a plot is shown.

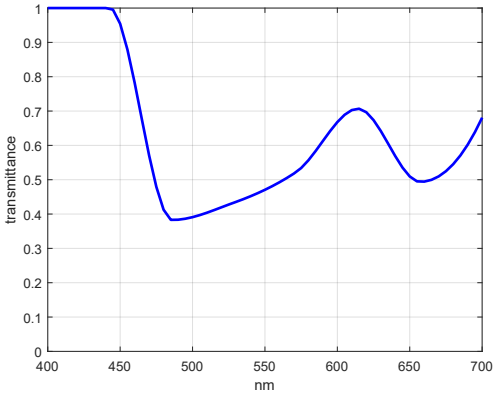

Figure 4. *Optimal filter maximizing the Vora value (Equation 20)*

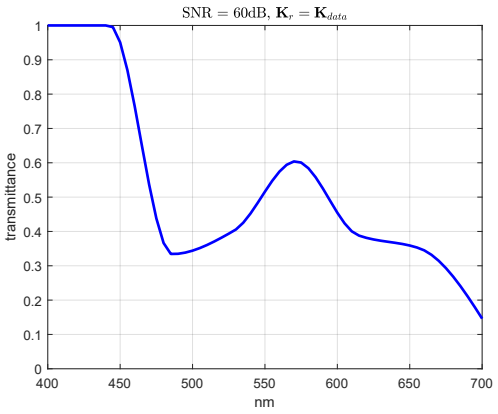

Figure 5. *Optimal filter solving Equation 21 at 60dB SNR and* $\mathbf{K}_r = \mathbf{K}_{data}$

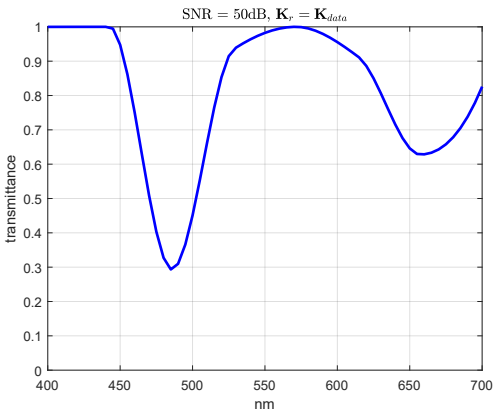

Figure 6. *Optimal filter solving Equation 21 at 50dB SNR and* $\mathbf{K}_r = \mathbf{K}_{data}$

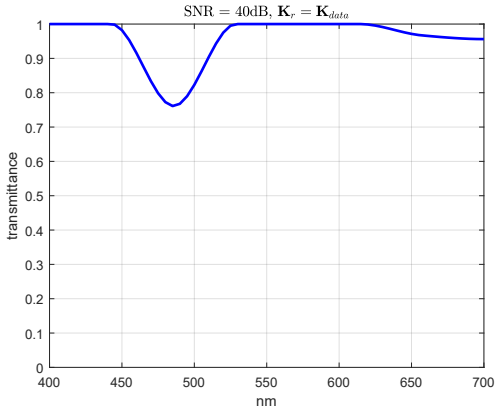

Figure 7. *Optimal filter solving Equation 21 at 40dB SNR and* $\mathbf{K}_r = \mathbf{K}_{data}$

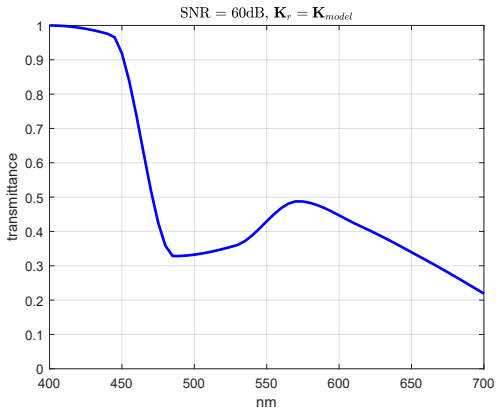

Figure 8. *Optimal filter solving Equation 21 at 60dB SNR and* $\mathbf{K}_r = \mathbf{K}_{model}$

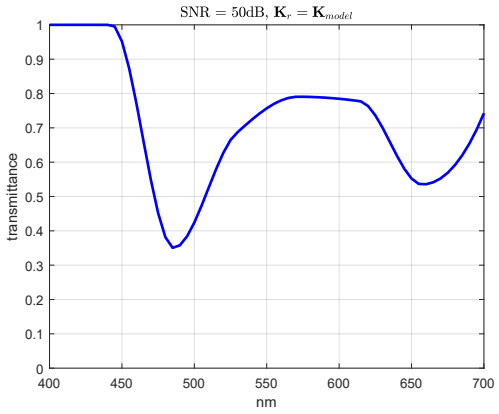

Figure 9. *Optimal filter solving Equation 21 at 50dB SNR and* $\mathbf{K}_r = \mathbf{K}_{model}$

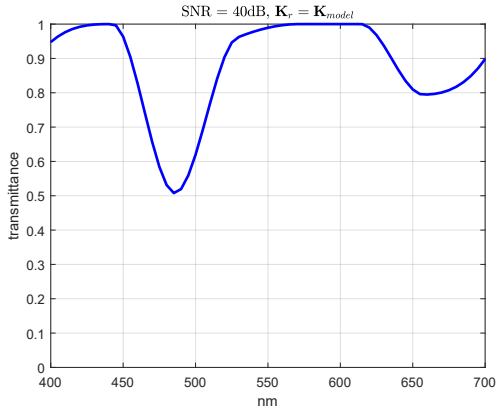

Figure 10. *Optimal filter solving Equation 21 at 40dB SNR and* $\mathbf{K}_r = \mathbf{K}_{model}$

Table 1: Mean square error results (scaled by 1000)

	$\mathbf{K}_r = \mathbf{K}_{data}$			$\mathbf{K}_r = \mathbf{K}_{model}$		
	40dB	50dB	60dB	40dB	50dB	60dB
No filter	2.02	1.20	1.04	2.23	1.45	1.31
Vora filter	2.80	1.16	0.79	2.89	1.33	1.01
40dB filter	**1.99**	1.12	0.96	**2.11**	1.19	1.02
50dB filter	2.08	**0.93**	0.71	2.39	**1.11**	0.86
60dB filter	3.23	1.18	**0.65**	3.4	1.33	**0.79**

Table 2: CIELAB ΔE differences

	$\mathbf{K}_r = \mathbf{K}_{data}$			$\mathbf{K}_r = \mathbf{K}_{model}$		
	40dB	50dB	60dB	40dB	50dB	60dB
No filter	**4.48**	1.92	1.25	**4.60**	2.12	1.50
Vora filter	6.79	2.35	0.94	6.9	2.42	**1.04**
40dB filter	4.54	1.86	1.13	4.82	**1.95**	1.19
50dB filter	5.00	**1.83**	**0.93**	5.71	2.07	**1.04**
60dB filter	7.54	2.59	1.01	8.20	2.81	1.06

Table 3: Effective SNR

	$\mathbf{K}_r = \mathbf{K}_{data}$			$\mathbf{K}_r = \mathbf{K}_{model}$		
	40dB	50dB	60dB	40dB	50dB	60dB
No filter	40	50	60	40	50	60
Vora filter	35.3	45.3	55.3	35.3	45.3	55.4
40dB filter	39.6	49.6	59.6	38.9	48.9	58.9
50dB filter	38.1	48.1	58.1	36.8	46.8	56.8
60dB filter	34.3	44.3	54.3	33.8	43.8	53.8

References

[1] D-Y. Ng and J. P. Allebach, "A subspace matching color filter design methodology for a multispectral imaging system," *IEEE Trans. Image Process.*, vol. 15, no. 9, pp. 2631-2643, (2006)

[2] Y. Monno, T. Kitao, M. Tanaka, and M. Okutomi, "Optimal spectral sensitivity functions for a single-camera one-shot multispectral imaging system," *2012 IEEE Int. Conf. Image Process.*, pp. 2137-2140, (2012)

[3] A. M. Nahavandi and M. A. Tehran, "A new manufacturable filter design approach for spectral reflectance estimation," *Color Res. & App.*, vol. 42, no. 3, pp. 316-326, June (2017)

[4] P. Xu and H. Xu, "Filter selection based on representative training samples for multispectral imaging," *Optik - Intern. J. for Light and Electron Optics*, vol. 127, no. 20, pp. 9743-9754, Oct. (2016)

[5] S.X. Li, "Filter selection for optimizing the spectral sensitivity of broadband multispectral cameras based on maximum linear independence," *Sensors*, vol. 18, pp. 1455, (2018)

[6] R. V. Kollarits and D. C. Gibbon, "Improving the color fidelity of cameras for advanced television systems," *SPIE Proc.*, vol. 1656, pp. 19-29, (1992)

[7] K. Engelhardt and P. Seitz, "Optimum color filters for CCD digital cameras," *Appl. Opt.*, vol. 32, no. 16, pp. 3015-3023, June (1993)

[8] M. J. Vrhel and H. J. Trussell, "Filter considerations in color correction," *IEEE Trans. Image Process.*, vol. 3, no. 2, pp. 147-161, (1994)

[9] M. J. Vrhel and H. J. Trussell, "Optimal color filters in the presence of noise," *IEEE Trans. Image Process.*, vol. 4, no. 6, pp. 814-823, (1995)

[10] G. Sharma, H. J. Trussell, and M. J. Vrhel, "Optimal nonnegative color scanning filters," *IEEE Trans. Image Process.*, vol. 7, no. 1, pp. 129-133, Jan. (1998)

[11] H. Kuniba and R. S. Berns, "Spectral sensitivity optimization of color image sensors considering photon shot noise," *J. Electron. Imag.*, vol. 18, no. 2, pp. 1-14, (2009)

[12] M. Wolski, C. Bouman, J. P. Allebach, and E. Walowit, "Optimization of sensor response functions for colorimetry of reflective and emissive objects," *IEEE Trans. Image Process.*, vol. 5, no. 3, pp. 507-517, (1996)

[13] M. J. Vrhel, H. J. Trussell, and J. Bosch, "Design and realization of optimal color filters for multi-illuminant color correction," *J. Electron. Imag.*, vol. 4, pp. 6-14, Jan. (1995)

[14] M. Parmar and S. J. Reeves, "Selection of optimal spectral sensitivity functions for color filter arrays," *IEEE Trans. Image Process.*, vol. 19, no. 12, pp. 3190-3203, (2010)

[15] H. J. Trussell, A. O. Ercan, and N. G. Kingsbury, "Color filters: When "optimal" is not optimal," *2016 IEEE Int. Conf. Image Process.* , Phoenix, AZ, pp. 3987-3991, (2016)

[16] P. L. Vora and H. J. Trussell, "Mathematical methods for the analysis of color scanning filters," *IEEE Trans. Image Process.*, vol. 6, no. 2, pp. 321-327, (1997)

[17] P. L. Vora and H. J. Trussell, "Mathematical methods for the design of color scanning filters," *IEEE Trans. Image Process.*, vol. 6, no. 2, pp. 312-320, (1997)

[18] P. L. Vora and H. J. Trussell, Measure of goodness of a set of color scanning filters," *J. Opt. Soc. Amer. A*, vol. 10, no. 7, pp. 1499-1508, (1993)

[19] H. E. J. Neugebauer, "Quality factor for filters whose spectral transmittances are different from color mixture curves, and its application to color photography," *J. Opt. Soc. Amer.*, vol. 46, pp. 821-824, Oct. (1956)

[20] G. Sharma and H. J. Trussell, "Figures of merit for color scanners," *IEEE Trans. Image Process.*, vol. 6, no. 7, pp. 990-1001, July (1997)

[21] S.Quan, N.Ohta,and N.Katoh,"Optimization of camera spectral sensitivities," in *Proc. IS&T SID 8th Color Imaging Conf.*, Scottsdale, AZ, pp. 273-278, (2000)

[22] P. Vora, "Inner products and orthogonality in color recording filter design," *IEEE Trans. Image Process.*, vol. 10, no. 4, pp. 632-642, Apr. (2001)

[23] G. D. Finlayson, Y. Zhu, and H. Gong, "Using a simple colour prefilter to make cameras more colorimetric," in *IS&T 26th Color and Imaging Conference*, pp. 182-186, (2018)

[24] G. D. Finlayson and Y. Zhu, "Finding a colour filter to make a camera colorimetric by optimisation," in *International Workshop on Computational Color Imaging.*, Springer, pp. 53-62, (2019)

[25] Y. Zhu and G. Finlayson, "An improved optimization method for finding a color filter to make a camera more colorimetric," in *Electronic Imaging 2020*. Society for Imaging Science and Technology, (2020)

[26] H. J. Trussell and M. S. Kulkarni, "Sampling and processing of color signals," *IEEE Trans. Image Process.*, vol. 5, no. 4, pp. 677-681, April (1996)

[27] R. Luther, Aus dem Gebiet der Farbreizmetrik, Zeitschrift fur Technische *Physik*, vol. 8, pp. 540-558, (1927)

[28] D. Wüller, "In situ measured spectral radiation of natural objects," *IS&T 17th Color and Imaging Conference*, pp. 159-163, November (2009)

[29] H. J. Trussell and R. Zhang, "The dominance of Poisson noise in color digital cameras," *2012 IEEE Int. Conf. Image Process.*, pp. 329-332, (2012)

Author Biography

Michael Vrhel was awarded his PhD from North Carolina State University in 1993; during his PhD, he was an Eastman Kodak Fellow. He has many years' experience working in digital imaging, including biomedical imaging and signal processing at NIH; color instrument and color software design at Color Savvy Systems Ltd, and positions at Conexant Systems, TAK Imaging and Artifex Software. A senior member of the IEEE, he has a number of current and pending patents and is the author of numerous papers in the areas of image and signal processing including a book, The Fundamanentals of Digital Imaging. His current interests include efficient computational color rendering methods as well as deep learning applications.